Supporting Information

Age-Dependent Rat Lung Deposition Patterns of Inhaled 20 Nanometer Gold Nanoparticles and their Quantitative Biokinetics in Adult Rats

Wolfgang G. Kreyling*[1,2], Winfried Möller[1†], Uwe Holzwarth[3], Stephanie Hirn[1], Alexander Wenk[1,5], Carsten Schleh[1,6], Martin Schäffler[1], Nadine Haberl[1], Neil Gibson[3], Johannes C. Schittny[4]

[1] Comprehensive Pneumology Center, Institute of Lung Biology and Disease, Helmholtz Zentrum München – German Research Center for Environmental Health, Ingolstaedter Landstrasse 1, D-85764 Neuherberg / Munich, Germany

[2] Institute of Epidemiology, Helmholtz Center Munich – German Research Center for Environmental Health, Ingolstaedter Landstrasse 1, D-85764 Neuherberg / Munich, Germany

[3] European Commission, Joint Research Centre, Directorate for Health, Consumers and Reference Materials, Via E. Fermi 2749, I-21027 Ispra (VA), Italy

[5] Current address: Dept. Infrastructure, Safety, Occupational Protection, Helmholtz Zentrum München – German Research Center for Environmental Health, D-85764 Neuherberg / Munich, Germany

[6] Current address: Abteilung Gesundheitsschutz, Berufsgenossenschaft Holz und Metall, Am Knie 8, D-81241 München, Germany

[4]Institute of Anatomy, University of Bern, Baltzerstrasse 2, CH-3012 Berne, Switzerland

† Dr. Winfried Möller is deceased

***Corresponding author**

Dr. Wolfgang G. Kreyling

Institute of Epidemiology

Helmholtz Centre Munich, German Research Center for Environmental Health

85764 Neuherberg / Munich, Germany

Email: kreyling@helmholtz-muenchen.de, Phone: +49-89-2351-4817

Content of supporting information

- Aerosol size distribution measurements using SMPS and spectral fitting
- Lung and body retention fits
- Intratracheal inhalation exposure to the freshly generated [^{195}Au]AuNP aerosol
- Age dependent [^{195}Au]AuNP deposition distribution
- Sample preparation for radiometric analysis of biokinetics
- Radiometric and statistical analysis
- BAL relative to CLR, relocation and re-entrainment
- Parameters of inhalation and deposition
- Total [^{195}Au]AuNP deposition in each rat determined by the balanced ^{195}Au activities of the entire dissected rat including its total excretion
- ^{195}Au activity determination of skeleton and soft tissue
- Blood correction and total blood volume
- [^{195}Au]AuNP accumulation and retention in secondary organs and tissues relative to translocated [^{195}Au]AuNP across the ABB
- [^{195}Au]AuNP concentration per mass of organ or tissues (1/g) as fractions of IPLD

- [^{195}Au]AuNP retention in the trachea and main bronchi

Aerosol size distribution measurements using SMPS and spectral fitting

For each two-hour inhalation exposure the [^{195}Au]AuNP size distribution was measured continuously by SMPS (scanning mobility particle spectrometer), resulting in about 40 spectra. The SMPS (consisting of a model 3071 differential mobility analyzer and a model 3010 CPC, TSI, Aachen, Germany) was operated at a main flow of 6 L/min and a sample flow of 0.6 L/min providing spectra in the range of 10 nm – 420 nm. CMD (count median diameter) and GSD (geometric standard deviation) were averaged and given as mean ± SD in Table 2. VMD (volumetric median diameter), as well as number concentrations and volume concentrations were averaged too. Since SMPS measurements were not provided below 10 nm, missing data were extrapolated in order to estimate the contribution of smaller nanoparticles to the size distribution. The extrapolation of spectral data was extended down to 1 nm size making use of an averaged spectrum over the 40 measured number size distributions and fitting the averaged spectrum to a lognormal size distribution minimizing the sum of least squares for the independent variables: median diameter, geometric standard deviation and spectral peak height. Since measured spectral data > 100 nm became noisy at the level below 10^{-4} of peak maximum, the fit was performed in the size range of 1 -100 nm.
These corrections led to slightly lower CMDs of about 19 nm instead of the 21 nm measured while the GSD changed only negligibly (Table 2). Changes of the VMD were also negligible.

Lung and body retention fits

Lung retention $LR(t)$ in Fig. S1A is based on the data obtained from the five dissection time points (Table 4: 1st line of "total lungs") which were fitted to a mono exponential function using a least squares algorithm resulting in

$$LR(t) = 0.977 \times \exp\left\{-\frac{t \times \ln 2}{23.3\,\mathrm{d}}\right\}. \qquad (1a)$$

For comparison the body retention, BR(t) of the 28d group of rats, in Fig. S1B is dominated by lung retention with minor contributions of the translocated fractions that are present in all secondary organs, tissues and blood (Table 4). It can be estimated from the excretion data between days 3 – 28 according to

$$BR(t) = 1 - \bar{a}_{\mathrm{faeces,cumul}}(t) - \bar{a}_{\mathrm{urine,cumul}}(t) \qquad t \in [3, 28\ \mathrm{d}] \qquad (1b)$$

where $\bar{a}_{\text{feces,cumul}}(t)$ and $\bar{a}_{\text{urine,cumul}}(t)$ denote the mean cumulative activity fractions of the 28d group of rats excreted up to time t *via* feces and urine, respectively. At least square fit of the body retention to a mono-exponential function gives

$$BR(t) = 0.963 \times \exp\left\{-\frac{t \times \ln 2}{27.8\ \text{d}}\right\} \qquad \text{t} \in [3, 28\ \text{d}] \qquad (1c)$$

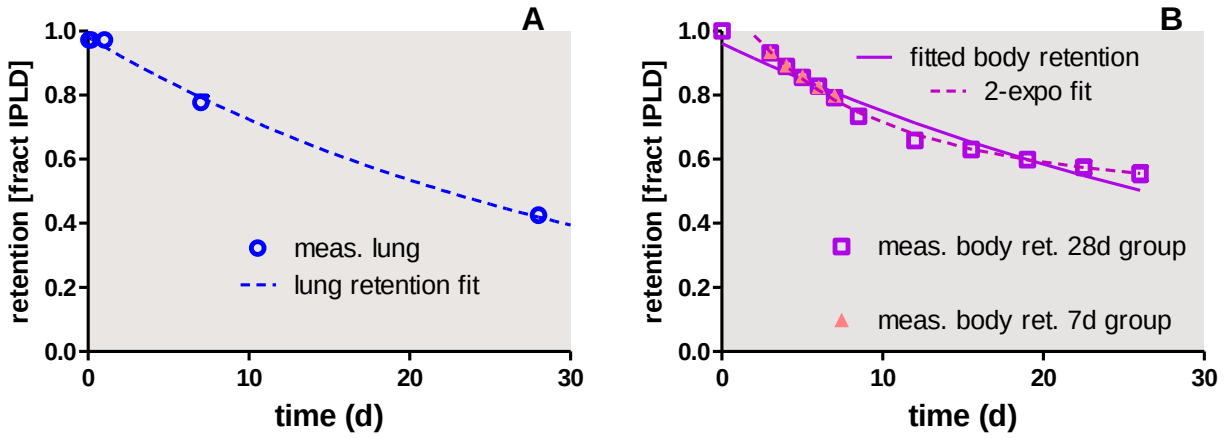

Figure S1: A: **Kinetics of mean lung retained fractions (per IPLD) obtained from five dissection time points (blue circles, data taken from Table 4) and exponential fit with half-life of 23.3 d. B: Mean body retention of the 28d group of rats from d3 to d28 (purple squares) calculated according to Eqn (1b) together with least squares fits to one exponential term (single exponential fit: half-life 27.8 d) and a double exponential fit (half-lives 4.9 d and 120 d). For comparison data from d3 to d7 obtained from the d7 group of rats are shown.**

While in Fig. S1A the fitted exponential term is essentially determined by three time points – day 1, day 7, day 28 – the fitted half-life of 23 d can only be a rough estimate. In contrast, the body retention in Fig. S1B provides more data points indicating that 12 days *p.e.* the data decrease more slowly than before. This is reflected in the slightly higher fitted half-life of 28 d. The body retention data between day 3 and day 7 of the 28d group of rats are very well confirmed by those of the 7d group of rats.

Intratracheal inhalation exposure to the freshly generated [^{195}Au]AuNP aerosol

As described earlier, [1, 2] four rats were anesthetized by an intramuscular injection of a mixture of Medetomidin (15 μg/100 g body weight), Midazolam (0.2 mg/100 g body weight), and Fentanyl (0.5 μg/100 g body weight). For endotracheal intubation of the adult rats a flexible cannula (16 G, 1.7 mm diameter, 50 mm length) was placed in the upper trachea under visual control and sealed against outside air with a modified pipette tip wedged gently into the laryngeal opening. [1-3] For 7d and 14d aged rats smaller flexible cannulas (G22, 0.9 mm diameter, 25 mm length and G20, 1.1 mm diameter, 32 mm length, respectively) were used. The animals were placed on their left lateral side in one of the four plethysmographs (50 mm diameter, 20 cm length, volume 390 cm³) of the inhalation apparatus and connected with the endotracheal cannula to the aerosol line outside of the plethysmograph. For 7d and 14d aged rats, smaller plethysmographs-boxes were used (30 mm diameter, 8 cm length volume 56 cm³and 40 mm diameter, 12 cm length, volume 150 cm³, respectively). Ventilation was computer controlled with a negative pressure of −1.5 kPa applied to the plethysmograph for 0.5 s of inspiration followed by 0.5 s spontaneous expiration at ambient air pressure, resulting in a breathing frequency of 60 min^{-1}. This ventilation pattern caused inspiration of about 75% of total rat lung capacity (TLC), so animals were slightly hyperventilated and did not breathe spontaneously but followed the computer-controlled breathing pattern, Fig. S2.

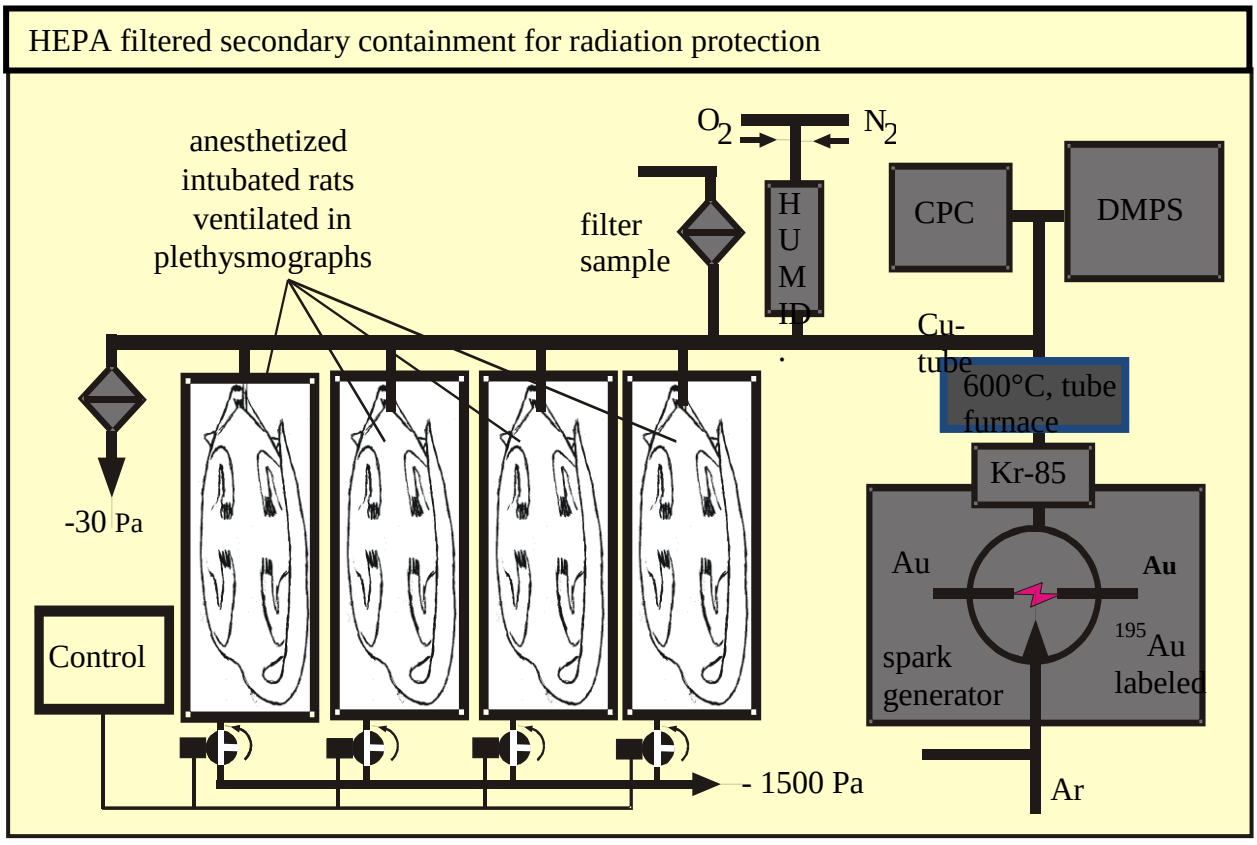

Figure S2: **Schematics of the spark ignition aerosol generator and the aerosol inhalation apparatus.**

Age dependent [^{195}Au]AuNP deposition distribution

The results of the age-dependent deposition experiments are presented in Fig. S3 which shows an increasing total deposited dose in the lungs with increasing age of the rats. Additionally, for all ages, the data clearly show a predominant deposition on the caudal region of both lungs as compared to the cranial lung regions. It should be noted that there is a caudal deposition minimum at an age of 21 d.

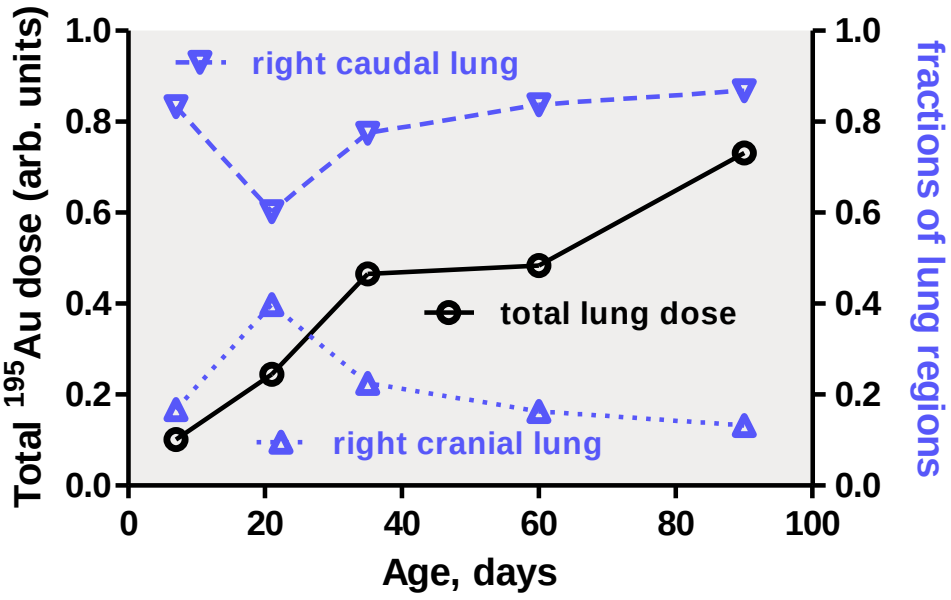

Figure S3: **Total deposited [^{195}Au]AuNP dose (circles) determined from SPECT imaging are shown together with the fractions of the caudal region (triangles down) and the cranial regions (triangles up) of the lungs of each rat.**

The deposition fractions obtained from the intratracheally inhaled (*i.e.* low-pressure ventilated and endotracheally intubated) rats were compared with the estimates provided by the MPPD Software (vs. 3.04) [4] shown in Fig. S4.

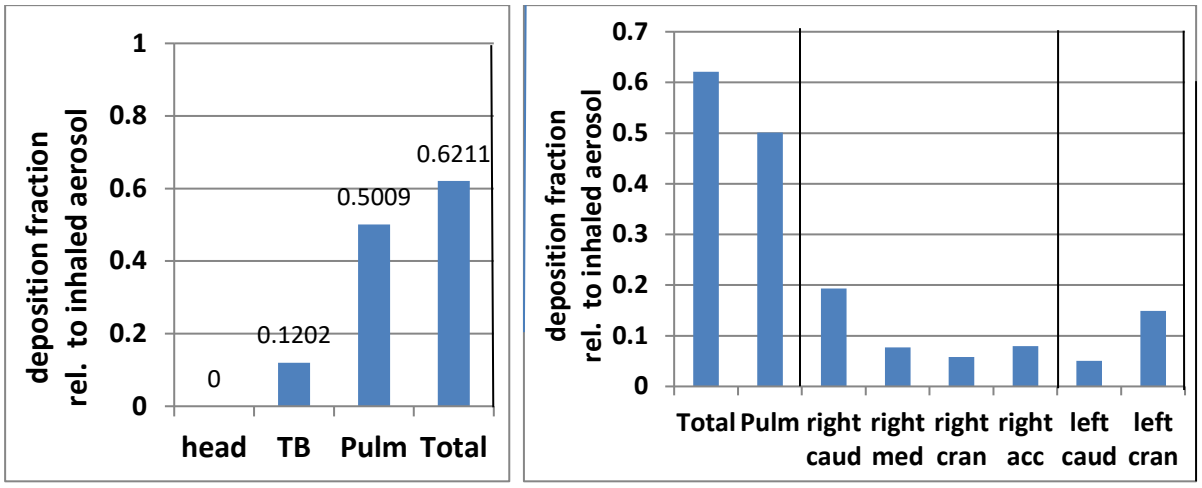

Figure S4: **Left: Total and regional deposition fractions in adult rats estimated by the MPPD Software (vs. 3.04) according to endotracheal breathing. Right: In addition lobar deposition fractions; the sum over all lobes yields total deposition. All MPPD model parameters are listed in Table S1; TB – deposited fraction in the tracheo-bronchial region, Pulm - deposited fraction in the pulmonary region, *i.e.* IPLD.**

The MPPD model does not provide age dependent deposition estimates for rats, but it provides regional (*i.e.* left and right lung) and lobar deposition data (*i.e.* caudal and cranial lobes). The corresponding deposition estimates of the MPPD model obtained are presented in the lower part of Table S1. In the upper part of Table S1 the input parameters used for the MPPD modeling are compiled. Since the MPPD model provides estimates when the rats are located during inhalation exposure on their left lateral side (as in our study), the model predicts twice as high deposition in the right lung compared to the left lung (Table S1, lower part) which is in qualitative agreement with the imaging results shown in Fig. 4. However, the model does not reproduce a similar inhomogeneity between the cranial *versus* the caudal deposition in the lungs as demonstrated by the experimental data in Fig. S3. This is most likely due to the negative pressure intratracheal inhalation causing predominant diaphragmatic ventilation which cannot be taken into account by the MPPD software package.

Table S1: Upper part: Model parameters used in the MPPD simulation. Lower part: Deposited fractions relative to total deposition in left *versus* right lung and in cranial *versus* caudal lungs.

MPPD model (version 3.04)		
Species & Model	**Physiology parameters**	**aerosol parameters**

species	adult Long Evans rat	TLC (cm^3)	13.7	CMD (µm)	0.022
geometry	assym. mult. path	FRC (cm^3)	4.0	GSD	1.6
exposure	endotracheal	breath frequency (min^{-1})	60	density ($g\ cm^{-3}$)	12
position	left lateral	TV (cm^3)	4.0	aspect ratio	1
		inspir. fract.	0.5	aerosol concen-tration ($mg\ m^{-3}$)	1.6
		pause	0		

parts of lungs	**lobes**	**deposition (rel. to total Deposition)**
caudal lungs	right caudal, right accessory, left caudal,	0.532
cranial lungs	right cranial, right medial, left cranial	0.468
right lungs	right caudal, right medial, right accessory, right cranial	0.672
left lungs	left caudal, left cranial	0.328

Sample preparation for radiometric analysis of biokinetics

At the chosen retention times of "immediately after inhalation" (1h), 4h, 24h, 7d or 28d after a 2-hour [^{195}Au]AuNP intratracheal inhalation, rats were anesthetized (by 5 % isoflurane inhalation) and euthanized by exsanguination *via* the abdominal aorta as described earlier. [1, 2, 5-7] [8] It should be noted that the time point immediately after the 2-hour inhalation is set to 1h, as the mean time available for the AuNP clearance and translocation during inhalation exposure corresponds to 1-hour. Approximately 70 % of the total blood volume could be recovered. Organs, tissues, carcass and excretions were collected for radiometric analysis (see Table S2). During dissection, none of the organs were cut and all fluids were cannulated (where necessary) in order to avoid any cross contamination. In addition, BAL (broncho-alveolar lavage) was performed. Organs, tissues, carcass and excretions were collected for radio-analysis (see Table S2).

Table S2: Organ, tissue and other samples prepared for radiometric analysis:

lungs*	trachea + main bronchi, incl. hilar lymph nodes	BAL cells*	BAL fluid*
$liver_{(2nd)}$	$spleen_{(2nd)}$	$kidneys_{(2nd)}$	
$brain_{(2nd)}$	$heart_{(2nd)}$	$uterus_{(2nd)}$	
GIT: gastro-intestinal tract, comprising esophagus, stomach, small and large intestine			

total skin$_{(2nd)}$	muscle sample$_{(2nd)}$	skinned head$_{(2nd)}$ without brain
exsanguinated blood sample$_{(2nd)}$		
bone sample$_{(2nd)}$ (humerus or femur carefully cleaned from soft tissue)		
carcass$_{(2nd)}$: total remaining carcass beyond the listed organs and tissues including the skeleton and soft tissue but excluding the skin		
Soft tissue: all tissues of the remaining carcass without skeleton		
Secondary organs$_{(2nd)}$: sum of all secondary organs indexed with $_{(2nd)}$.		
excretion: total daily urine and feces, collected separately; in the 28-day group integral urinary *versus* fecal excretion was collected over 3-4 days as described above		

* Lavaged lungs; BAL; separation of BAL cells from BAL fluid supernatant by centrifugation as described in [8]. Total lungs represent the sum of [^{195}Au]AuNP in lavaged lungs and in BAL.

$_{(2nd)}$ The index "$_{(2nd)}$" indicates those secondary organs and tissues in which [^{195}Au]AuNP may accumulate after translocation across the ABB into blood circulation.

Of the group of rats used to study the age-dependent deposition distribution only the microwave-dried lungs were analyzed by γ-spectrometry but no other secondary organs, fluids or tissues.

Radiometric and statistical analysis

The ^{195}Au radioactivity of all samples was measured by γ-ray spectrometry without any further physico-chemical sample preparation in either a lead-shielded 10-mL or a lead-shielded 1-L well type NaI(Tl) scintillation detector as previously described. [2, 5-7 8] For radiometric analysis the 99 keV γ-ray emission was used; see further details at [9]. The count rates were corrected for physical decay and background radiation. Additionally, count rates were calibrated to a ^{195}Au reference source. For this purpose a [^{195}Au]AuNP filter sample of 350 Bq (at reference date) was used whose activity was

determined by an absolutely calibrated Ge/Li semiconductor detector. The ^{195}Au radioactivity was converted into the mass of the [^{195}Au]AuNP making use of the fixed ratio 1.55 MBq/mg that was determined for the activated electrode tips. Samples yielding net counts (*i.e.*, background-corrected counts) in the 99 keV region-of-interest of the ^{195}Au γ-ray spectrum were defined to be below the detection limit when they were less than three standard deviations of the background count rate in this region-of-interest without any sample in the detector well.

For a complete balance of the administered ^{195}Au radioactivity within each rat, the ^{195}Au activities of all individual samples were summed up for each rat and used as a denominator for the calculation of the percentage of ^{195}Au activity fraction in each sample. These fractions were averaged over the four rats of each group and are reported with the SEM as described earlier. [1, 2, 5-7, 8]

All calculated significances are based on a One-Way-ANOVA test and a *post hoc* Bonferoni Test. In case of an individual two group comparison, the unpaired t-test was used. Significance was considered at $p \leq 0.05$.

BAL relative to CLR , relocation and re-entrainment

Serial BAL of rat lungs were performed at each time point of sacrifice to assess [^{195}Au]AuNP retention on the lung epithelium as free [^{195}Au]AuNP suspended in the BAL-fluid or associated with freely moving BAL-cells or as [^{195}Au]AuNP relocated from the epithelial surface either bound and/or taken up by cells of the epithelial barrier and interstitial sites. BAL was performed by applying 6 x 5 ml of phosphate-buffered-saline (PBS without Ca^{2+} or Mg^{2+}) under gentle massage of the thorax. The recovered BALF (about 80% of instilled PBS) was centrifuged at 500 g for 20 min at room temperature to separate the lavaged BAL-cells from the supernatant. The [^{195}Au]AuNP content was determined by γ-ray-spectrometry. At each BAL the total number of lavaged cells was acquired using a hemocytometer by a dilution of the spun-down cells and trypan-blue staining. For cell differentiation cyto-centrifuged slide preparations of the lavaged cells were Wright-Giemsa stained for each sacrificed animal (see Fig. S5). The slightly increased neutrophil fractions over the first 24-hour, indicating a transient inflammatory response, may have been caused by the methodology of the 2-hour intratracheal inhalation at a high [^{195}Au]AuNP aerosol concentration *via* the endotracheal catheter being placed into the upper third of the trachea.

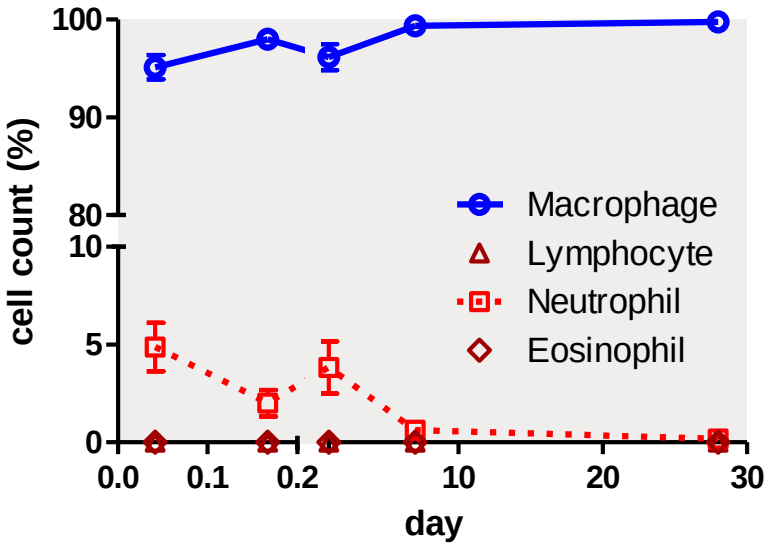

Figure S5: **Percentage of BAL cell differentiation at each time point of sacrifice. Mean ± SEM; n≥4.**

By γ-ray-spectrometry the fractions of free [^{195}Au]AuNP in the BALF and of [^{195}Au]AuNP in BALC and in the lavaged lungs were determined. Applying this BAL procedure we obtained about 4 * 10^6 macrophages per BAL which is in average very similar to our previous studies.[1, 2, 10] Normalizing the number of totally recovered macrophages of each BAL by the mean number of the total surface macrophage population of (12.5 ± 0.8) * 10^6 previously determined in the lungs of WKY rats [10] we estimated the total fraction of [^{195}Au]AuNP associated with lung surface macrophages (AM pool).

[^{195}Au]AuNP fractions in BALC and BALF are snapshots of currently retained [^{195}Au]AuNP on the epithelium resulting from the dynamics of arriving AuNP due to the interstitial re-entrainment and clearance of [^{195}Au]AuNP by LT-MC. (Note, in Fig. 6B daily LT-MC per CLR is shown). When normalizing these fractions a_i at time t_i by the contemporary [^{195}Au]AuNP lung retention (CLR) at time t_i, the obtained fractions are independent of earlier nanoparticulate clearance. These fractions are shown in Fig. 8. The fraction of free [^{195}Au]AuNP in BALF is about 0.20 of the total [^{195}Au]AuNP in lungs immediately *p.e.*. However, it drops very rapidly below 0.01 within the first 24-hours *p.e.*. In contrast, the macrophage-associated [^{195}Au]AuNP fraction per CLR is about 0.10 of total [^{195}Au]AuNP in the lungs starting from 4 hours until the end of the study (data not shown). Since the number of the lavaged AM in BALC are less than in the entire AM pool in the lungs, the fractions in the AM-pool [10] are plotted in Fig. 8 showing rather constant [^{195}Au]AuNP fractions of about 0.2. These data are very similar to the 28d-average fraction of 0.2 for 20 nm [^{192}Ir]IrNP within the AM pool taken from our previous reports [2, 10] and represented by the dashed line in Fig. 8. In our previous report we

concluded that only a small fraction per CLR (~0.2) of 20 nm IrNP was internalized in the total AM pool at each time point while the remaining fraction of about 0.8 per CLR was already bound and/or taken up by cells of the epithelial barrier and/or the interstitial space. Interestingly, this pattern was quite the opposite to that of 2.1 µm PSL particles and 1.3 µm fused-alumino-silicate particles (FAP) which remained predominantly (~0.8) in the total AM pool on the epithelial surface throughout the entire observation period of six months. [10-12] Note [^{195}Au]AuNP in AM were continuously eliminated *via* AM migration towards the mucociliary escalator and out of the lungs. The fraction of 0.2 in AM remained constant since retention in the AM pool and also the [^{195}Au]AuNP fraction was not accessible to BAL but retained within the epithelium and interstitium. Material differences may play an additional role, but also the tendency to form NP agglomerates. This needs further investigation which will follow in our next report on the biokinetics after inhalation of 20 nm TiO_2NP.

Parameters of inhalation and deposition

In the following we use the index i to distinguish individual rats that are subjected to inhalation exposure of [^{195}Au]AuNP for a duration of two hours in a group of animals labeled by the index j that were sacrificed after a certain retention period ("immediately after inhalation" (1h), 4h, 24h, 7d and 28d).

During each inhalation exposure of a group j of rats a [^{195}Au]AuNP aerosol sample was collected on a filter, and the [^{195}Au]Au activity $A_{\mathrm{filt}}^{\mathrm{j}}$ (in Bq) on the filter was determined by γ-spectrometry. The aerosol volume $V_{\mathrm{filt}}^{\mathrm{j}}$ (L) was measured with a gas flow meter and the specific aerosol activity $a_{\mathrm{filt}}^{\mathrm{j}}$ (in Bq/L) was calculated as

$$a_{\mathrm{filt}}^{\mathrm{j}} = A_{\mathrm{filt}}^{\mathrm{j}} / V_{\mathrm{filt}}^{\mathrm{j}} \qquad \mathrm{j} = 1,2,3,4,5 \qquad (2)$$

The mean total lung capacity (TLC) in mL of healthy, female WKY-Kyoto Wistar rats was determined by [13] to be $TLC = 0.047 \cdot BW$ (*BW*= body weight in gram). At a ventilation-pressure of -1.5 kPa the tidal volume $TV_{\mathrm{i}}^{\mathrm{j}}$ of each intubated rat i of group j was set at 75% TLC, which gives

$$TV_{\mathrm{i}}^{\mathrm{j}} = 0.75 \cdot TLC_{\mathrm{i}}^{\mathrm{j}} = 0.75 \cdot 0.047 \cdot BW_{\mathrm{i}}^{\mathrm{j}} \qquad \mathrm{i} = 1,2,3\ldots;\ \ \mathrm{j} = 1,2,3,4,5 \qquad (3)$$

The rats were ventilated for a ventilation time t_{inhal} of two hours at a ventilation rate $f_{\mathrm{i}}^{\mathrm{j}}$ of 60 min^{-1} set by the computer-controlled inhalation apparatus. The inhaled aerosol volume $V_{inhal,i}^{j}$ of each rat i of group j was calculated as

$$V_{\mathrm{inhal,i}}^{\mathrm{j}} = f_{\mathrm{i}}^{\mathrm{j}} \cdot TV_{\mathrm{i}}^{\mathrm{j}} \cdot t_{\mathrm{inhal}} \qquad \mathrm{i} = 1,2,3..\,\mathrm{rats};\ \mathrm{j} = 1..5\ \mathrm{group} \qquad (4)$$

Total [^{195}Au]AuNP deposition in each rat determined by the balanced ^{195}Au activities of the entire dissected rat including its total excretion

The inhaled aerosol activity $A_{\mathrm{inhal,i}}^{\mathrm{j}}$ is calculated from the product of the total inhaled volume $V_{\mathrm{inhal,i}}^{\mathrm{j}}$ determined from Eqn (4) and the specific ^{195}Au aerosol activity $a_{\mathrm{filt}}^{\mathrm{j}}$ (in Bq/L) (Eqn (2) as

$$A_{\mathrm{inhal,i}}^{\mathrm{j}} = V_{\mathrm{inhal,i}}^{\mathrm{j}} \cdot a_{\mathrm{filt}}^{\mathrm{j}} \qquad \mathrm{i} = 1,2,3\ \ldots\ \mathrm{rats};\ \mathrm{j} = 1..5\ \mathrm{group} \qquad (5)$$

In order to determine the initially deposited [^{195}Au]AuNP activity $A(\mathrm{ILD})_{\mathrm{i}}^{\mathrm{j}}$ (Bq) in the lungs of each rat (*i.e.* ILD), which is smaller than the inhaled dose because a significant amount of nanoparticles are exhaled again, all γ-spectrometrically measured sample activities $A_{\mathrm{sample\ k,i}}^{\mathrm{j}}$ were summed up, where the index k identifies all specimens (all samples of organs, tissues, total excretion of rat (i,j)) collected from a single animal i of group j according to

$$A(\mathrm{ILD})_{i}^{j} = \sum_{\mathrm{k=1}}^{\mathrm{n}} A_{\mathrm{sample\ k,i}}^{\mathrm{j}} \qquad \mathrm{k} = 1..\mathrm{n};\ \text{all samples of organs, tissues, total excretion of rat (i,j)} \qquad (6)$$

$$\mathrm{i} = 1,2,3\ \ldots\ \mathrm{rats};\ \mathrm{j} = 1..5\ \mathrm{group}$$

For the total deposited AuNP mass $m(\mathrm{ILD})_{\mathrm{i}}^{\mathrm{j}}$ (in µg) and AuNP number $N(\mathrm{ILD})_{\mathrm{i}}^{\mathrm{j}}$ the total deposited [^{195}Au]AuNP activity $A(\mathrm{ILD})_{\mathrm{i}}^{\mathrm{j}}$ of each rat was divided by the specific ^{195}Au activity concentration per Au mass (1.55 kBq/µg) or divided by the quotient of the specific aerosol activity $a_{\mathrm{filt}}^{\mathrm{j}}$ (Eqn. 2) and the averaged aerosol number concentration $N(\mathrm{Aer})_{\mathrm{i}}^{\mathrm{j}}$ (Table 2) determined by the CPC 3022A, respectively.

$$m(\mathrm{ILD})_i^j = A(\mathrm{ILD})_i^j / (1.55\,\mathrm{MBq/mg}) \quad (7a)$$

$$N(\mathrm{ILD})_i^j = N(\mathrm{Aer})_i^j \frac{A(\mathrm{ILD})_i^j}{a_{\mathrm{filt},i}^j} \quad \mathrm{i} = 1,2,3..\,\mathrm{rats};\ \mathrm{j} = 1..5\ \mathrm{group} \quad (7b)$$

In addition, the deposited [^{195}Au]AuNP activity fraction $a(\mathrm{ILD})_i^j$ was determined relative to the total inhaled aerosol activity of each rat according to Eqn (8).

$$a(\mathrm{ILD})_i^j = \frac{A(\mathrm{ILD})_i^j}{V_{\mathrm{inhal},i}^j \cdot a_{\mathrm{filt}}^j} \quad \mathrm{i} = 1,2,3..\,\mathrm{rats};\ \mathrm{j} = 1..5\ \mathrm{group} \quad (8)$$

In the next step [^{195}Au]AuNP activity fractions in organs and tissues (index k) $a(\mathrm{ILD})_{\mathrm{sample\,k,i}}^j$ with respect to the deposited dose in the lungs were calculated by normalizing all measured sample activities $A_{\mathrm{sample\,k,i}}^j$ (Bq) to the total deposited ^{195}Au activity $A(\mathrm{ILD})_{\mathrm{sample\,k,i}}^j$ (Bq) of each rat (i,j) according to

$$a(\mathrm{ILD})_{\mathrm{sample\,k,i}}^j = \frac{A_{\mathrm{sample\,k,i}}^j}{A(\mathrm{ILD})_i^j} \quad \mathrm{i} = 1,2,3..\,\mathrm{rats};\ \mathrm{j} = 1..5\ \mathrm{group}$$

k = 1..n; all samples of organs, tissues, total excretion of rat (i,j) (9)

MCC of [^{195}Au]AuNP from thoracic airways after intratracheal inhalation was considered to contribute negligibly to the translocation across the ABB. Therefore, for calculations of [^{195}Au]AuNP translocation across the ABB, MCC was excluded from the complete balance by subtracting the ^{195}Au -radioactivity contributions of the head (without brain), trachea, GIT, and feces obtained during the first 2-3 days *p.e.* from the overall radioactivity balance of each animal and normalizing the activities determined in all other organs and tissues to the new (reduced) balance. Thus, the amount of intratracheally inhaled material at time $t = 0$ that is available for translocation through the ABB is reduced due to MCC within the first 48h after instillation by

$$A(\mathrm{ILD})_{\mathrm{MCC,i}}^j = A(\mathrm{ILD})_{\mathrm{head-brain,i}}^j + A(\mathrm{ILD})_{\mathrm{trachea,i}}^j + A(\mathrm{ILD})_{\mathrm{GIT,i}}^j + A(\mathrm{ILD})_{\mathrm{feces,i}}^j \quad (10)$$

$$a(\mathrm{ILD})^{\mathrm{j}}_{\mathrm{MCC,i}} = \frac{A(\mathrm{ILD})^{\mathrm{j}}_{\mathrm{MCC,i}}}{A(\mathrm{ILD})^{\mathrm{j}}_{\mathrm{i}}} \qquad \mathrm{i} = 1,2,3..\,\mathrm{rats};\ \mathrm{j} = 1..5\ \mathrm{group} \qquad (11)$$

Where $A(\mathrm{ILD})^{\mathrm{j}}_{\mathrm{head-brain,i}}\,(t; t \le 24\mathrm{h})$ denotes the ^{195}Au activity determined for the head without the brain, $A(\mathrm{ILD})^{\mathrm{j}}_{\mathrm{trachea,i}}\,(t; t \le 24\mathrm{h})$ the ^{195}Au activity in the trachea, $A(\mathrm{ILD})^{\mathrm{j}}_{\mathrm{GIT,i}}\ (t; t \le 48\mathrm{h})$ the one in the gastro-intestinal tract and $A(\mathrm{ILD})^{\mathrm{j}}_{\mathrm{feces,i}}\ (t; t \le 48\mathrm{h})$ the activity of the feces collected during the first 48-hours.

For the estimation of the [^{195}Au]AuNP activity deposited on the alveolar epithelium $A(\mathrm{IPLD})^{\mathrm{j}}_{\mathrm{i}}$ the fast cleared MCC activity $A(\mathrm{ILD})^{\mathrm{j}}_{\mathrm{MCC,i}}$ is subtracted from the total deposited [^{195}Au]AuNP activity $A(\mathrm{ILD})^{\mathrm{j}}_{\mathrm{i}}$ determined according to Eqn (6), thus, the activity of the initial peripheral lung dose and the corresponding activity fraction $a(\mathrm{IPLD})^{\mathrm{j}}_{\mathrm{i}}$ normalized to the total initially deposited activity $A(\mathrm{ILD})^{\mathrm{j}}_{\mathrm{i}}$ are

$$A(\mathrm{IPLD})^{\mathrm{j}}_{\mathrm{i}} = A(\mathrm{ILD})^{\mathrm{j}}_{\mathrm{i}} - A(\mathrm{ILD})^{\mathrm{j}}_{\mathrm{MCC,i}} \qquad \mathrm{i} = 1,2,3..\,\mathrm{rats};\ \mathrm{j} = 1..5\ \mathrm{group} \qquad (12)$$

$$\tilde{a}(\mathrm{IPLD})^{\mathrm{j}}_{\mathrm{i}} = \frac{A(\mathrm{ILD})^{\mathrm{j}}_{\mathrm{i}} - A(\mathrm{ILD})^{\mathrm{j}}_{\mathrm{MCC,i}}}{A(\mathrm{ILD})^{\mathrm{j}}_{\mathrm{i}}}$$

For any calculations of translocated fractions across the ABB all sample fractions $\tilde{a}(\mathrm{IPLD})^{\mathrm{j}}_{\mathrm{sample\ k,i}}$ are normalized to $A(\mathrm{IPLD})^{\mathrm{j}}_{\mathrm{i}}$ according to

$$\tilde{a}(\mathrm{IPLD})^{\mathrm{j}}_{\mathrm{sample\ k,i}} = \frac{A^{\mathrm{j}}_{\mathrm{sample\ k,i}}}{A(\mathrm{IPLD})^{\mathrm{j}}_{\mathrm{i}}} \qquad \begin{array}{r}\mathrm{i} = 1,2,3..\,\mathrm{rats};\ \mathrm{j} = 1..5\ \mathrm{group}\\ \mathrm{k} = 1..\mathrm{n};\ \text{all samples of organs, tissues,}\\ \text{total excretion of rat (i,j)}\end{array} \qquad (13)$$

where the symbol $\tilde{a}$ is used to emphasis that the normalization is done to a reduced balance as the activity which is cleared by fast mucociliary clearance $A(\mathrm{ILD})^{\mathrm{j}}_{\mathrm{MCC,i}}$ is no longer available for translocation through the ABB.

To estimate the long-term cleared [^{195}Au]AuNP fraction cleared by LT-MC from the alveolar epithelium to the mucociliary escalator of the conducting airways, the total fecal excretion is calculated by summing up all fecal samples from day 3 up to day m (d_m).

$$\tilde{a}^{j}_{LT-MC,i} = \sum_{l=1}^{m} a^{j}_{feces,l,i} \qquad \begin{array}{l} l = 1,\ldots m\,;\ d_m \in [3,\ldots 28\ \text{day}] \\ i = 1,2,3..\,\text{rats};\ j = 1..5\ \text{group} \end{array} \tag{14}$$

MCC and LT-MC are derived from the ^{195}Au activity measured in fecal excretions, which exhibits a delay due to the time required for the passage through the GIT. This time delay causes an uncertainty when defining the time after which MCC is essentially concluded. Fecal excretions measured after 2 days are completely assigned to LT-MC which also starts immediately after inhalation and should therefore be extrapolated down to time zero. However, due to the inevitable uncertainties in determining MCC it appears exaggerated to further correct MCC for a minor contribution of early LT-MC to the fecal excretion data. Our dissection data indicate that MCC is nearly completed already after 4 hours which is for sure much faster than the conventional estimate of 24-hoursused in literature. [29]

^{195}Au activity determination of skeleton and soft tissue

The ^{195}Au activity in the whole skeleton of each rat $A^{j}_{skeleton,j}$ was extrapolated from the activity of a bone sample $A^{j}_{bone\ sample,i}$ and its mass $m^{j}_{bonesample,i}$ assuming the estimated weight of the skeleton to be 10% [14] of the total body weight $m^{j}_{tot\ body,i}$

$$A^{j}_{skeleton,j} = A^{j}_{bonesample,i} \cdot \frac{m_{totbody,i}}{m_{bonesample,i}} \cdot 0.1 \qquad i = 1,2,3..\,\text{rats};\ j = 1..5\ \text{group} \tag{15}$$

For this purpose the bone sample was carefully cleaned from other tissue. The ^{195}Au activity to be assigned to the soft tissue $A^{j}_{soft\text{-}tissue,i}$ of each rat was calculated from the difference of the ^{195}Au-

radioactivity content of the total remaining carcass $A_{\text{carcass,i}}$ (including soft tissue, muscle sample, skeleton, bone sample) and the activity in the skeleton as determined in Eqn (15) as

$$A^{\text{j}}_{\text{soft-tissue,i}} = A^{\text{j}}_{\text{carcass,i}} - A^{\text{j}}_{\text{skeleton,i}} \qquad \text{i} = 1,2,3..\text{rats};\ \text{j} = 1..5\ \text{group} \qquad (16)$$

Blood correction and total blood volume

In order to obtain the true value of ^{195}Au activity in the organs and tissues of interest the radioactivity contributed by the residual blood retained after exsanguination had to be subtracted. In the case of the carcass, the difference between the estimated total blood volume of the animal and the sum of all organ blood contents and the collected blood sample was calculated to be the blood volume of the carcass.

Table S2: Organ specific weight factors $f^{\text{Oeff}}_{\text{organ,i}}$ for the residual blood in the organ tissue after exsanguination given as residual blood weight per organ weight according to Oeff & König. [15]

Lung ($g \bullet g^{-1}$)	liver ($g \bullet g^{-1}$)	spleen ($g \bullet g^{-1}$)	kidney ($g \bullet g^{-1}$)	brain ($g \bullet g^{-1}$)
0.28 ± 0.10)	0.14 ± 0.03	0.16 ± 0.04	0.22 ± 0.04	0.018 ± 0.001
heart ($g \bullet g^{-1}$)	GIT[§] ($g \bullet g^{-1}$)	muscle ($g \bullet g^{-1}$)	fat ($g \bullet g^{-1}$)	thyroid* g/organ
0.15 ± 0.02	0.020 ± 0.006	0.016 ± 0.002	0.012 ± 0.002	0.008 ± 0.001

* thyroid given for complete organ; [§] intestine and stomach

The blood contents of organs and tissues were calculated according to the findings of Oeff and Konig [15] shown in Table S2 and the ^{195}Au radioactivities of the organs were corrected for these values as

$$A^{\text{j}}_{\text{organ}_\text{k}\text{,i}} = A^{\text{measured,j}}_{\text{organ}_\text{k}\text{,i}} - A^{\text{blood correction,j}}_{\text{organ}_\text{k}\text{,i}} \qquad \text{i} = 1,2,3..\text{rats};\ \text{j} = 1..5\ \text{group} \qquad (17)$$

where $A^{measured}_{organ_k,i}$ denotes the ^{195}Au activity measured in the organ "k" of rat $_{i,j}$ (i = 1,2,3 … rats; j = 1…5 group for retention times of 1h, 4h, 24h, 7d and 28d) in (Bq) which is corrected for the residual blood content by subtracting $A^{bloodcorrection,j}_{organ_k,i}$ calculated according to

$$A^{blood\,correction,j}_{organ_k,i} = \frac{A^{measured,j}_{bloodsample,i} \cdot m^{measured,j}_{organ_k,i} \cdot f^{Oeff}_{organ_k}}{m^{measured,j}_{bloodsample,i}} \qquad \begin{matrix} i = 1,2,3..rats; \\ j = 1..5\ group \end{matrix} \qquad (18)$$

making use of the mass $m^{measured,j}_{bloodsample,i}$ and the activity $A^{measured,j}_{bloodsample,i}$ measured for the blood recovered from exsanguination, the mass of the organ $m^{measured,j}_{organ_k,i}$ and the organ specific weight factor $f^{Oeff}_{organ_k}$ for the residual blood in the organ tissue according to Oeff and Koenig.[15] The total blood volume *BV* (in cm³) was estimated to be

$$BV = 0.06 \cdot BW + 0.77 \qquad (19)$$

according to the work of Lee and Blaufox, [16] where *BW* denotes the body weight (in g).

To determine the ^{195}Au activity in the residual blood of the remaining carcass or skeleton for each rat the following procedure was applied. Firstly, the mass of the residual blood volume in the carcass or skeleton $m^{res.-blood,j}_{tiss_k,i}$ ($tiss_k$ ∈ [carcass, skeleton]) was calculated by subtracting from the mass of the total blood volume m_{BV} the mass of the sampled blood volume $m^{j}_{meas.-bloodsample,i}$ and the sum of the masses of the residual blood volumes of all organs $m^{res.-blood,j}_{organ_k,i}$ according to [15]

$$m^{res.-blood,j}_{tiss_k,i} = m_{BV} - m^{j}_{meas.-bloodsample,i} - \sum_{l \neq k} m_{organ_l,i} \cdot f^{Oeff}_{organ_l,i} \qquad \begin{matrix} i = 1,2,3..rats; \\ j = 1..5\ group \end{matrix} \qquad (20)$$

For each rat the ^{195}Au activity in the residual blood of the remaining carcass or skeleton $A^{blood\,correction}_{tiss_k}(i,j)$ ($tiss_k$ ∈ [carcass, skeleton]) is then given by

$$A^{res.-blood,j}_{tiss_k,i} = \frac{A^{j}_{meas.-bloodsample,i}}{m^{j}_{meas.-bloodsample,i}} \cdot m^{res.-blood,j}_{tiss_k,i} \cdot \frac{m_{tiss_k,i}}{m^{j}_{BW,i}} \qquad \begin{matrix} i = 1,2,3..rats; \\ j = 1..5\ group \end{matrix} \qquad (21)$$

as the ^{195}Au activity concentration determined from the blood sample taken times the mass of the residual blood in carcass or skeleton times the mass fraction of carcass or skeleton with respect to the rat's body weight. This estimate assumes that the residual blood volume is proportional to the

mass of either the carcass or skeleton. Since the remaining carcass consists of the skeleton and soft tissue, the ^{195}Au activity in the residual blood of the soft tissue is the difference between ^{195}Au activities of residual blood of carcass minus that of skeleton given by

$$A^{\text{res.-blood,j}}_{\text{soft-tissue,i}} = A^{\text{res.-blood,j}}_{\text{carcass,i}} - A^{\text{res.-blood,j}}_{\text{skeleton,i}} \qquad \text{i} = 1,2,3..\,\text{rats};\ \text{j} = 1..5\ \text{group} \qquad (20)$$

To determine the contribution of the ^{195}Au activity in the residual blood to the total ^{195}Au activity retained in all organs and tissues, the ratio

$$RB^{\text{blood correction, j}}_{\text{organ}_k\text{, i}} = \frac{A^{\text{blood correction, j}}_{\text{organ}_k\text{, i}}}{A^{\text{j}}_{\text{meas.-organ}_k\text{, i}}} \qquad \text{i} = 1,2,3..\,\text{rats};\ \text{j} = 1..5\ \text{group} \qquad (21)$$

is defined, where the ^{195}Au activity of the residual blood retained in each organ, $A^{\text{blood correction, j}}_{\text{organ(k),i}}$, is calculated according to Eqn (18). As the retention of ^{195}Au activity in blood, organs and tissues depends on time and follows different patterns the ratio $RB^{\text{blood correction, j}}_{\text{organ(k),i}}$ itself depends on time. This is shown in Fig. S6 for all organs, remaining carcass, skeleton and soft tissue.

The corrections are from the very beginning very small since the dominant part of the [^{195}Au]AuNP was retained in the (lavaged) lungs and the ^{195}Au activity concentration in blood was very low. Corrections of the order of 10% are only seen for organs that retain very small activity fractions, where even small corrections for activity retained in the residual blood make greater contributions.

Meaningful corrections are derived for heart, brain, kidneys, uterus and skeleton. Corrections for liver, spleen and soft tissues that heavily accumulate [^{195}Au]AuNP are rather small after the onset of nanoparticle clearance.

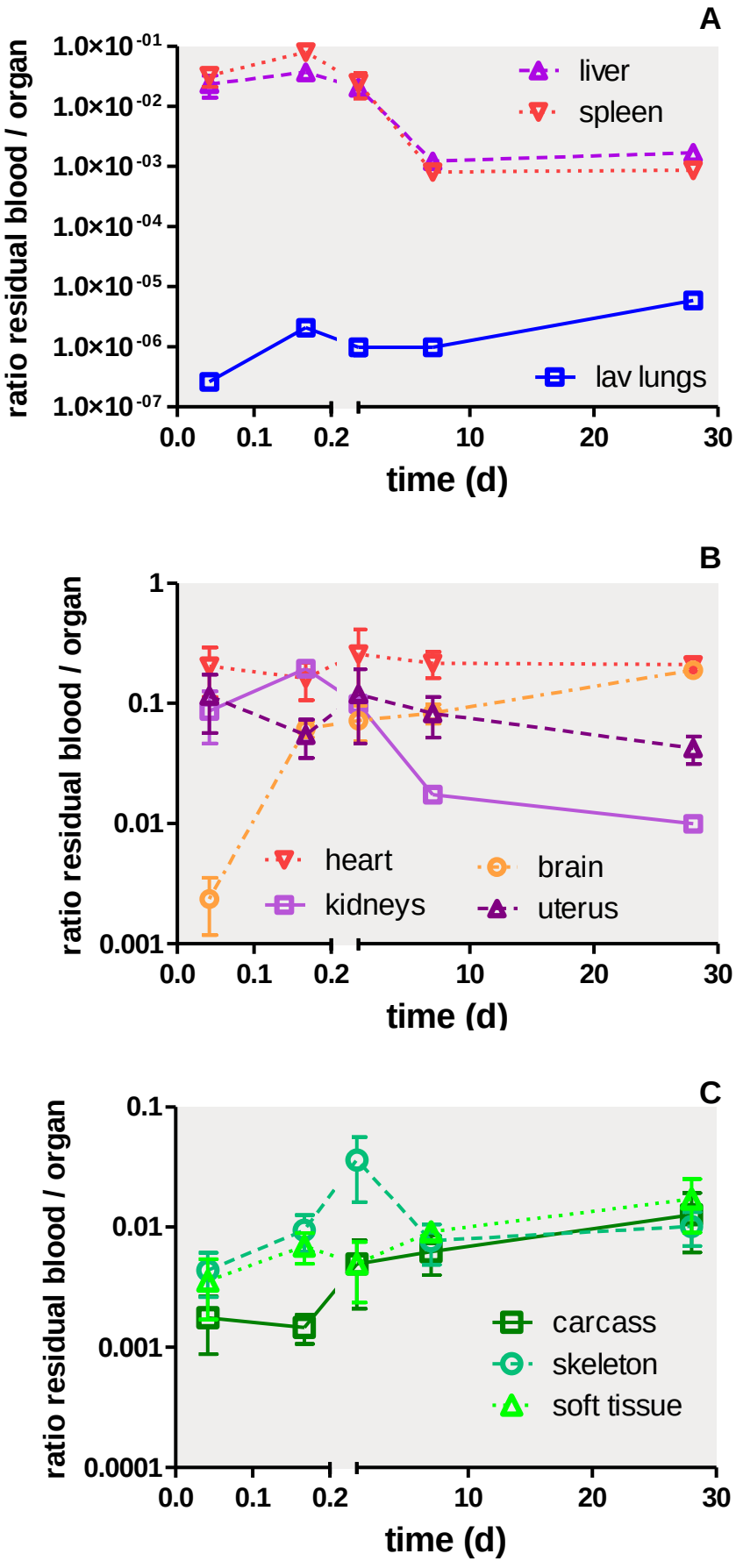
A
ratio residual blood / organ
1.0×10-01
1.0×10-02
1.0×10-03
1.0×10-04
1.0×10-05
1.0×10-06
1.0×10-07
liver
spleen
lav lungs
0.0
0.1
0.2
10
20
30
time (d)
B
ratio residual blood / organ
1
0.1
0.01
0.001
heart
kidneys
brain
uterus
0.0
0.1
0.2
10
20
30
time (d)
C
ratio residual blood / organ
0.1
0.01
0.001
0.0001
carcass
skeleton
soft tissue
0.0
0.1
0.2
10
20
30
time (d)

Figure S6: **Ratio $RB_{\text{organ, i}}^{\text{blood correction}}$ of the ^{195}Au activity in the residual blood over the measured organ or tissue activity. A: lavaged lungs, liver, spleen; B: kidneys, heart, brain, uterus; C: carcass, skeleton, soft tissue. Mean ± SEM, n ≥ 4 rats per time point.**

[^{195}Au]AuNP accumulation and retention in secondary organs and tissues relative to translocated [^{195}Au]AuNP across the ABB

In order to determine the amount of [^{195}Au]AuNP in secondary organs and tissues as a fraction of [^{195}Au]AuNP that crossed the ABB, we have to normalize all activity values measured for all secondary organs and tissues $A^{\text{j}}_{\text{2ndorgan,i}}(t)$, all urine samples $A^{\text{j}}_{\text{urine,i}}(t)$ and all blood samples $A^{\text{j}}_{\text{bloodsample,i}}$ to a value which is smaller than the value $A(t=0)=A_0$ that has been deposited after the 2-hour intratracheal inhalation. The normalization activity $A^{\text{j}}_{\text{t-loc,i}}$ is the sum of all $A^{\text{j}}_{\text{2ndorgan,i}}(t)$, $A^{\text{j}}_{\text{urine,i}}(t)$, $A^{\text{j}}_{\text{bloodsample,i}}(t)$. Therefore,

$$A^{\text{j}}_{\text{t-loc,i}} = \sum_{\text{k=1}}^{\text{n}} A^{\text{j,k}}_{\text{2ndorgan,i}} + \sum_{\text{l=1}}^{\text{o}} A^{\text{j,l}}_{\text{bloodsample,i}} + \sum_{\text{m=1}}^{\text{p}} A^{\text{j,m}}_{\text{urine,i}} \qquad (24)$$

$\text{i} = 1,2,3..\text{rats};$

$\text{j} = 1..5\ \text{group}$

k=1,2..n; 2nd organs

l=1,2..o; blood sample

m=1,2..p; urine sample

holds for all rats i in each group j, which will be referred to as the translocated dose, which is a specific value for each rat used in the five retention time groups. The fractions of [^{195}Au]AuNP that has been accumulated in organs and tissues k, blood l and urine m after passing the ABB can now be determined for each rat by normalizing the activities $A^{j}_{\text{organ}_\text{k},\text{i}}$ according to

$$\hat{a}^{j}_{\text{organ}_\text{k},\text{i}} = \frac{A^{j}_{\text{organ}_\text{k},\text{i}}}{A^{\text{j}}_{\text{t-loc,i}}}$$

$$\hat{a}^{j}_{\text{blood}_\text{l},\text{i}} = \frac{A^{j}_{\text{blood}_\text{l},\text{i}}}{A^{\text{j}}_{\text{t-loc,i}}} \qquad (25)$$

$\text{i} = 1,2,3..\text{rats};\ \text{j} = 1..5\ \text{group}$

k=1,2..n; 2nd organs

l=1,2..o; blood sample

$$\hat{a}^{j}_{\text{urine}_m,\text{i}} = \frac{A^{j}_{\text{urine}_m,\text{i}}}{A^{\text{j}}_{\text{t-loc,i}}}$$ m=1,2..p; urine sample

Note, all urinary samples and the slow macrophage-mediated [^{195}Au]AuNP fractions from days > 2 during the remaining retention time are included in the sum for normalization since both are considered to be part of the clearance and translocation.

[^{195}Au]AuNP concentration per mass of organ or tissues (1/g) as fractions of IPLD

While for biokinetics and dosimetry it is more convenient to present and discuss [^{195}Au]AuNP fractions per total organ or tissue, the presentation of [^{195}Au]AuNP fractions per weight of organ or tissue as presented in Fig. S7 is more meaningful for toxicological considerations. Remarkably, [^{195}Au]AuNP concentration fractions per organ weight are similar in liver, spleen and kidneys suggesting similar concentrations of MPS cells. The concentrations start rather low at about 1×10^{-5} g^{-1} (Fig. S7A+C and Table 4). After four hours the [^{195}Au]AuNP concentrations begin to steeply increase in all three organs until day 7, followed by a moderate increase up to 7×10^{-4} g^{-1} , 14×10^{-4} g^{-1} , 2×10^{-4} g^{-1} , respectively, until day 28. Although most of the [^{195}Au]AuNP were found in soft tissue (Fig. 9 A+C and Table 4), the [^{195}Au]AuNP concentration in soft tissue (Fig. S7D and Table 4) is initially only one order of magnitude higher than in the three organs due to the large mass of soft tissue. Therefore, since [^{195}Au]AuNP concentrations in soft tissue decline over time, they become much lower than those of liver, spleen and kidneys after 28 days.

Fig. S7A shows that liver and spleen are the main secondary organs rapidly accumulating [^{195}Au]AuNP with still increasing values between day 7 and 28. Fig. S7B demonstrates that even organs that are well protected by barriers retain [^{195}Au]AuNP and that the heart exhibits a pronounced retention maximum after 24h. Fig. S7C shows that the [^{195}Au]AuNP concentration in the blood almost steadily increases by one order of magnitude throughout the observation period. Fig. S7D indicates that the highest concentrations during the first 24-hoursare built up in soft tissue which decrease thereafter while highest [^{195}Au]AuNP concentrations are obtained in liver and spleen. Note the soft tissue compartment does not only comprise lymphatic drainage and the vascular system but also MPS cells, all of which may contribute to [^{195}Au]AuNP retention. The retention in bone is much lower, but the evolution of the [^{195}Au]AuNP concentration in the skeleton follows the tendency observed in blood indicating that accumulation there is related to perfusion.

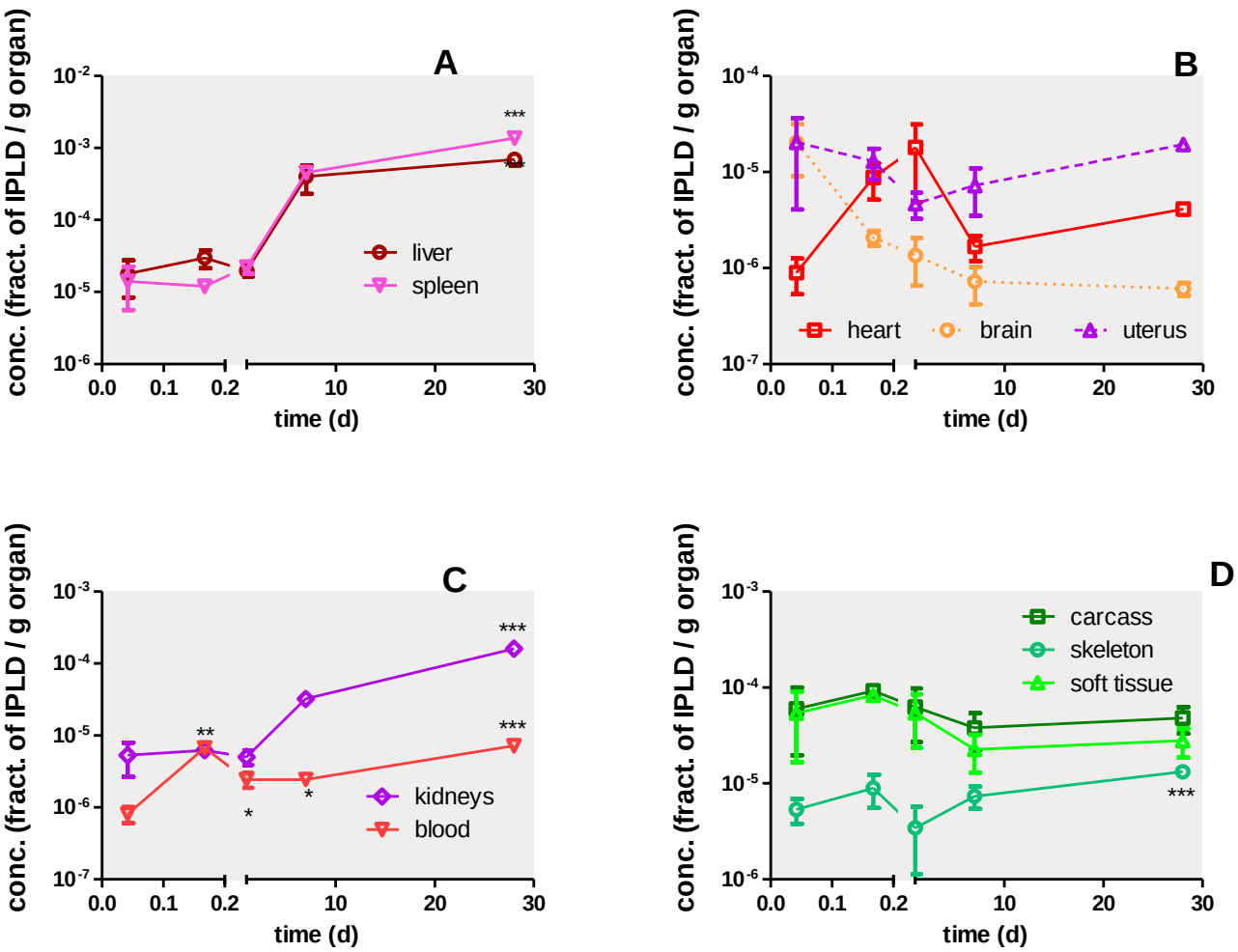

Figure S7: **Kinetics of [^{195}Au]AuNP concentrations per weight of organ or tissue: liver and spleen (A), heart, uterus and brain (B), kidneys and total blood (C) carcass, skeleton and soft tissue (D). Data are corrected for [^{195}Au]AuNP retained in the residual blood volume of organs and tissues; data are mean ± SEM; n ≥ 4 rats per time point. Statistical significances: p<0.05 (*), p<0.01 (**), p<0.001 (***); Panel A: *** 28d *vs.* all other times; Panel C: *** 28d *vs.* all other times; ** 0h *vs.* 4h; * 4h *vs.* 24h and 7d; Panel D: *** 28d *vs.* all other times.**

[^{195}Au]AuNP retention in the trachea and main bronchi

There are three options for accumulating [^{195}Au]AuNP in the trachea, first bifurcation and first bronchi:

1. Transient passage of [^{195}Au]AuNP on the mucociliary escalator
2. [^{195}Au]AuNP accumulation and retention in tracheobronchial and hilar lymph nodes

3. [^{195}Au]AuNP retention in cells of the epithelium

Regarding 1) there is continuous [^{195}Au]AuNP transport towards the larynx resulting initially from mucociliary clearance of [^{195}Au]AuNP which had been deposited on the epithelium of conducting airways. Thereafter, LT-MC of [^{195}Au]AuNP continues at a rate $r_{LT\text{-}MC}$ of 0.02 – 0.03 /d of the contemporary lung burden from peripheral sites of the lungs.[2, 10, 17] Hence, the [^{195}Au]AuNP amount transient in the dissected trachea and first bronchi can be estimated from the Wistar/Kyoto rat tracheal mucus velocity v_{TMV} of 1.9 mm/min [18] and the length of the trachea l_{tr} (28 mm) and first bronchi l_{br} (4 mm). Assuming a constant and continuous LT-MC transport rate and using the above mentioned transport rate $r_{LT\text{-}MC}$, the fractional amount f_{tr} corresponds to the [^{195}Au]AuNP residence time t_{res} within the trachea and bronchi divided by 1440 min of one day:

$$f_{tr} = r_{LT\text{-}MC} \times t_{res} / 1440\ \text{min} \qquad \text{with } t_{res} = (l_{tr} + l_{br}) / v_{TMV} \qquad (26)$$

Hence, t_{res} = 17 min and the range of fractional [^{195}Au]AuNP amounts f_{tr} are [0.00024, 0.00036] for dissections at 7d and 28d. Thus, the estimated amount of transitional [^{195}Au]AuNP in the tracheal sample from 7d to 28d retention is about tenfold lower compared to the measured data of Table 4 indicating that the contribution of [^{195}Au]AuNP in transit can only be associated with 10% of the [^{195}Au]AuNP in the tracheal sample.

Since MCC is time dependent, the estimate of the actual [^{195}Au]AuNP fraction in the tracheal sample during the first time points 1h, 4h and 24h cannot be precisely estimated. As shown in Table 3, immediately after the 2h-inhalation (named 1h retention time point) about 4% of the initially deposited [^{195}Au]AuNP had arrived in the GIT after having been swallowed indicating that MCC is in progress. (Note, MCC might even be retarded because the endotracheal tube may have compromised the ciliated action in the upper trachea during the inhalation exposure.) However, four hours later already >80% of the MCC fraction (*i.e.* sum of fecal excretion during day 1+2 averaged over all rats of the 7d and the 28d group) had reached the GIT of the rats of the 4h group (Table 3). At 24-hours *p.e.* the MCC fraction had increased only marginally against the 4-hours value. Therefore, the transient [^{195}Au]AuNP fractions in the tracheal sample after 24-hours and likewise after 4-hours are mainly determined by the long-term AM-mediated clearance rate, $r_{LT\text{-}MC}$ yielding similar fractional amount f_{tr} in the tracheal sample as those estimated for the 7d and 28d rats: f_{tr} = [0.00024, 0.00036]. Compared to the measured 4h and 24h tracheal sample data of Table 4 the transitional [^{195}Au]AuNP in the tracheal sample are about 40-fold lower indicating that the contribution of [^{195}Au]AuNP in transit can again only explain a tiny part of the [^{195}Au]AuNP observed. Hence, the observed amount of [^{195}Au]AuNP in the tracheal samples ought to be associated to either hilar lymph node retention

and/or epithelial retention in the trachea and main bronchi as discussed at the end of the Discussion section of the main paper.

References

1. Kreyling, W. G.; Semmler, M.; Erbe, F.; Mayer, P.; Takenaka, S.; Schulz, H.; Oberdörster, G.; Ziesenis, A., Translocation of Ultrafine Insoluble Iridium Particles from Lung Epithelium to Extrapulmonary Organs Is Size Dependent but Very Low. J. Toxicol. Environ. Health-Part A, **2002**,*65*, 1513-1530.
2. Semmler, M.; Seitz, J.; Erbe, F.; Mayer, P.; Heyder, J.; Oberdorster, G.; Kreyling, W. G., Long-Term Clearance Kinetics of Inhaled Ultrafine Insoluble Iridium Particles from the Rat Lung, Including Transient Translocation into Secondary Organs. *Inhalation Toxicol.* **2004**, *16*, 453-459.
3. Osier, M.; Oberdorster, G., Intratracheal Inhalation Vs Intratracheal Instillation: Differences in Particle Effects. *Fundam. Appl. Toxicol.* **1997**, *40*, 220-227.
4. (A.R.A.), A. R. A., Multiple-Path Particle Dosimetry Model (MPPD Version 3.0). 2009.
5. Hirn, S.; Semmler-Behnke, M.; Schleh, C.; Wenk, A.; Lipka, J.; Schaffler, M.; Takenaka, S.; Moller, W.; Schmid, G.; Simon, U.; Kreyling, W. G., Particle Size-Dependent and Surface Charge-Dependent Biodistribution of Gold Nanoparticles after Intravenous Administration. *Eur. J. Pharm. Biopharm.* **2011**, *77*, 407-416.
6. Kreyling, W. G.; Hirn, S.; Möller, W.; Schleh, C.; Wenk, A.; Celik, G.; Lipka, J.; Schäffler, M.; Haberl, N.; Johnston, B. D.; Sperling, R.; Schmid, G.; Simon, U.; Parak, W. J.; Semmler-Behnke, M., Air–Blood Barrier Translocation of Tracheally Instilled Gold Nanoparticles Inversely Depends on Particle Size. *ACS Nano* **2014**, *8*, 222 - 223.
7. Schleh, C.; Semmler-Behnke, M.; Lipka, J.; Wenk, A.; Hirn, S.; Schaffler, M.; Schmid, G.; Simon, U.; Kreyling, W. G., Size and Surface Charge of Gold Nanoparticles Determine Absorption across Intestinal Barriers and Accumulation in Secondary Target Organs after Oral Administration. *Nanotoxicology* **2012**, *6*, 36-46.
8. Kreyling, W. G.; Hirn, S.; Moller, W.; Schleh, C.; Wenk, A.; Celik, G.; Lipka, J.; Schaffler, M.; Haberl, N.; Johnston, B. D.; Sperling, R.; Schmid, G.; Simon, U.; Parak, W. J.; Semmler-Behnke, M., Air-Blood Barrier Translocation of Tracheally Instilled Gold Nanoparticles Inversely Depends on Particle Size. *ACS Nano* **2014**, *8*, 222-233.
9. Möller, W.; Gibson, N.; Geiser, M.; Pokhrel, S.; Wenk, A.; Takenaka, S.; Schmid, O.; Bulgheroni, A.; Simonelli, F.; Kozempel, J.; Holzwarth, U.; Wigge, C.; Eigeldinger-Berthou, S.; Mädler, L.; Kreyling, W., Gold Nanoparticle Aerosols for Rodent Inhalation and Translocation Studies. *J. Nanopart. Res.* **2013**, *15*, 1-13.
10. Semmler-Behnke, M.; Takenaka, S.; Fertsch, S.; Wenk, A.; Seitz, J.; Mayer, P.; Oberdorster, G.; Kreyling, W. G., Efficient Elimination of Inhaled Nanoparticles from the Alveolar Region: Evidence for Interstitial Uptake and Subsequent Reentrainment onto Airways Epithelium. *Environ. Health Perspect.* **2007**, *115*, 728-733.
11. Lehnert, B. E.; Valdez, Y. E.; Tietjen, G. L., Alveolar Macrophage-Particle Relationships During Lung Clearance. *Am. J. Respir. Cell Mol. Biol.* **1989**, *1*, 145-154.
12. Ellender, M.; Hodgson, A.; Wood, K. L.; Moody, J. C., Effect of Bronchopulmonary Lavage on Lung Retention and Clearance of Particulate Material in Hamsters. *Environ. Health Perspect.* **1992**, *97*, 209-213.

13. Bolle, I.; Eder, G.; Takenaka, S.; Ganguly, K.; Karrasch, S.; Zeller, C.; Neuner, M.; Kreyling, W. G.; Tsuda, A.; Schulz, H., Postnatal Lung Function in the Developing Rat. *J. Appl. Physiol.* **2008**, *104*, 1167-1176.
14. Charkes, N. D.; Brookes, M.; Makler, P. T., Jr., Studies of Skeletal Tracer Kinetics: Ii. Evaluation of a Five-Compartment Model of [18f]Fluoride Kinetics in Rats. *J. Nucl. Med.* **1979**, *20*, 1150-1157.
15. Oeff, K.; Konig, A., [Blood Volume of Rat Organs and Residual Amount of Blood after Blood Letting or Irrigation; Determination with Radiophosphorus-Labeled Erythrocytes.]. *Naunyn-Schmiedebergs Arch. Exp. Pathol. Pharmakol.* **1955**, *226*, 98-102.
16. Lee, H. B.; Blaufox, M. D., Blood Volume in the Rat. *J. Nucl. Med.* **1985**, *26*, 72-76.
17. Kreyling, W. G., Interspecies Comparison of Lung Clearance of "Insoluble" Particles. *J. Aerosol Med.* **1990**, *3*, S93-S110.
18. Felicetti, S. A.; Wolff, R. K.; Muggenburg, B. A., Comparison of Tracheal Mucous Transport in Rats, Guinea Pigs, Rabbits, and Dogs. J. Appl. Physiol.: Respir., Environ. Exercise Physiol. **1981**, *51*, 1612-1617.